Self-organized molecular-sized, hexagonally ordered SnO_x nanodot superlattices on Pt(111)

Cite as: Appl. Phys. Lett. **78**, 2766 (2001); https://doi.org/10.1063/1.1369613
Submitted: 15 August 2000 . Accepted: 05 March 2001 . Published Online: 25 April 2001

Matthias Batzill, David E. Beck, and Bruce E. Koel

Self-organized molecular-sized, hexagonally ordered SnO_x nanodot superlattices on Pt(111)

Matthias Batzill, David E. Beck, and Bruce E. Koel[a)]
Department of Chemistry, University of Southern California, Los Angeles, California 90089-0482

(Received 15 August 2000; accepted for publication 5 March 2001)

Complete oxidation of the $(\sqrt{3}\times\sqrt{3})R30°$ Sn/Pt(111) surface alloy or submonolayer amounts of Sn adatoms on Pt(111) under ultrahigh vacuum conditions, forms a highly ordered, lateral superlattice of SnO_x islands on the Pt(111) substrate. The island superstructure exhibits a sharp (5×5) low energy electron diffraction pattern. Scanning tunneling microscopy images show islands arranged in a hexagonal lattice, uniformly distributed over the whole sample. This island array is thermally stable up to 1050 K. The coincidence of the island periodicity with a multiple of the supporting substrate, and the same hexagonal symmetry of islands and substrate, suggests a strong island–substrate interaction. We propose that the island formation results from the breakup of a strained SnO_x adlayer. © *2001 American Institute of Physics.* [DOI: 10.1063/1.1369613]

Solid state structures of nanoscale dimensions may posses unique electronic, chemical, and physical properties. To exploit these properties, a method for their fabrication is required. Standard lithography methods lack the resolution to form structures smaller than ~10 nm and scanning probe based techniques are generally too slow to pattern large surface areas. Self-assembly is a promising approach to form large arrays of nanostructures with a narrow size distribution. Minimization of the free energy of a commensurately grown adlayer may result in the formation of uniformly sized islands in order to reduce the strain energy.[1] Another strain-relief mechanism for heteroepitaxially grown adlayers is the formation of regular arrays of dislocation lines.[2–4] It was demonstrated that these dislocation line patterns can be used as templates to grow ordered metal islands.[5,6] Similarly, long-range surface reconstructions may be used as a template with preferential nucleation sites for adatoms. Consequently, islands can be grown with the periodicity of the surface reconstruction of the substrate.[7,8] These island structures are, however, not stable at elevated temperatures. Here, we demonstrate that oxidation of the $(\sqrt{3}\times\sqrt{3})R30°$ Sn/Pt(111) surface alloy, or of a submonolayer Sn-film on Pt(111), results in the formation of uniformly distributed, highly ordered SnO_x island structures that are thermally stable up to 1050 K in ultrahigh vacuum (UHV). The work presented here has implications for the formation of nanostructures and the preparation of thin oxide films on metal substrates which has become of increasing interest in recent years.[9–11]

All of the experiments presented here were performed in an UHV apparatus with a base pressure of 2×10^{-10} Torr. For sample preparation, the apparatus was equipped with an ion gun, resistively heated Sn-evaporation source, and precision leak valves for gas dosing. The Pt(111) single crystal was heated by means of electron bombardment. The temperature of the sample was measured using a chromel/alumel thermocouple spotwelded to the side of the crystal. For sample characterization, the apparatus was equipped with a home-built scanning tunneling microscope (STM) following the design of Mugele and co-workers,[12] a cylindrical mirror analyzer for Auger electron spectroscopy (AES), and rear-view low energy electron diffraction (LEED) optics. In addition, the UHV chamber was equipped with a quadrupole mass spectrometer for residual gas analysis and temperature programmed desorption studies.

The Pt(111) single crystal was cleaned by standard procedures, consisting of cycles of 500 eV Ar^+ ion sputtering followed by annealing in a background of 2×10^{-7} Torr O_2 at 1000 K with a final annealing in UHV to 1200 K. The cleanliness of the sample was monitored by AES and the procedure was repeated until no contamination of the surface could be detected. The Sn deposition rate was calibrated by means of AES uptake plots. From these measurements, we estimated that the deposition rate used was 0.01 ML/s. We checked the Sn coverage by measuring the Sn (430 eV) to Pt (237 eV) peak-to-peak ratios in AES after each deposition of Sn. In order to form a $(\sqrt{3}\times\sqrt{3})R30°$ Sn/Pt(111) surface alloy $\Theta_{Sn}=0.9$ ML was deposited at room temperature and subsequently annealed to 1000 K for 10 s.[13] To oxidize the alloy surfaces or the Sn adlayers under UHV conditions, NO_2 was used as a clean, effective oxidant. The sample surface was saturated with oxygen by dosing NO_2 for 40 s at a background pressure of 4×10^{-8} Torr NO_2 and a sample temperature of 400 K. This temperature was chosen to avoid NO adsorption on the surface.[14] After dosing NO_2, the sample was flash annealed to its target temperature and the surfaces formed were characterized.

Oxidation of a submonolayer amount (~0.4 ML) of a Sn adlayer and subsequent annealing to 800–1000 K forms a surface structure exhibiting a (4×4) LEED pattern. This ordered structure was also confirmed by STM measurements. In the STM images, protrusions were seen that were separated by twice the Pt(111) surface lattice constant. However, every second spot in every second row was missing thus giving rise to a (4×4) unit cell as shown in Fig. 1(a). Although the composition of these protrusions cannot be determined from the STM images alone, we speculate that they

a)Electronic mail: koel@chem1.usc.edu

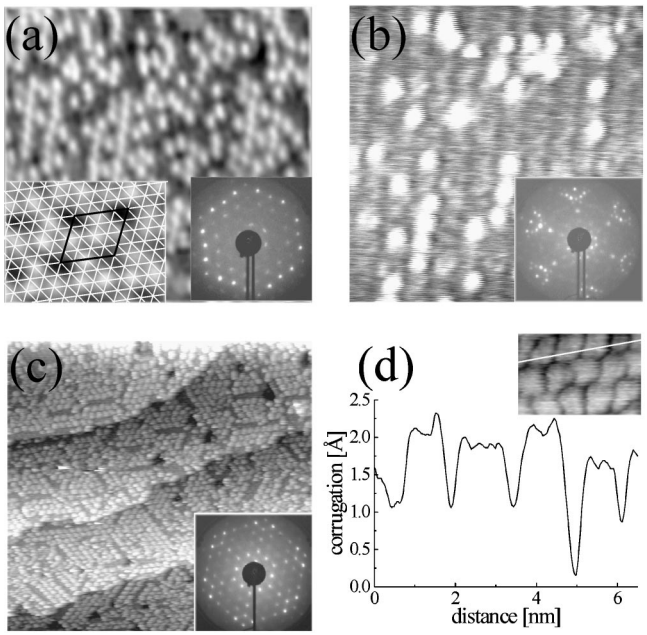

FIG. 1. (a) STM image (12 nm×12 nm) of a surface showing a (4×4) LEED pattern. The inset on the left-hand side shows a STM image at higher resolution of a well-ordered area on the surface. The white lines indicate the Pt-substrate lattice; the (4×4) unit cell is also highlighted. The inset on the right-hand side shows the (4×4) LEED pattern from this surface. (b) STM image (20 nm×20 nm) of the ''intermediate'' surface structure. The inset shows the LEED pattern from this surface. (c) STM image (62 nm×62 nm) of a (5×5) SnO_x island structure. The atomic steps in the image are similar to those observed on the clean Pt(111) substrate. The inset shows the (5×5) LEED pattern from this surface. (d) Higher resolution STM image (6.7 nm×3.3 nm) of the SnO_x island structure and cross section through the line indicated in the STM image.

represent SnO or Sn_2O species bound to a preferential Pt lattice site.

Similar results were obtained for oxidation of the $(\sqrt{3}\times\sqrt{3})R30°$ Sn/Pt surface alloy, although flash annealing to 860–880 K yielded a different surface structure. The LEED pattern and the STM data for this surface are shown in Fig. 1(b). Annealing this surface above 900 K, or annealing to 850 K for several minutes, results again in the (4×4) structure. AES data show that the Sn(430 eV):O(510 eV) ratio is increased for the (4×4) structure to a value of 4.8 compared to the structure formed by flashing the sample to 900 K where Sn(430 eV):O(510 eV)=3.6. Since we know from temperature programmed desorption studies that no oxygen desorbs in this temperature regime and that a small amount of subsurface tin is necessary to form the $(\sqrt{3}\times\sqrt{3})R30°$ Sn/Pt surface alloy, we conclude that the change in the Sn/O ratio is due to Sn segregation from the bulk to the surface. Sn segregation, being a thermally activated process, also explains why it takes several minutes to form the (4×4) at 850 K while it forms rapidly above 900 K. From these observations, we propose that the (4×4) structure is a Sn-enriched oxide, i.e., the Sn at the surface is not completely oxidized.

After obtaining the (4×4) structure, one may attempt to oxidize this surface again in order to more fully oxidize the SnO_x adlayer. This was done by repeating the oxidation procedure outlined previously. After the second NO_2 exposure and subsequent annealing, the more oxygen-rich surface was the more frequently observed structure [identical to Fig. 1(b)]. Although no structural differences between this film and the one depicted in Fig. 1(b) could be observed with LEED and STM, a smaller Sn(430 eV):O(510 eV) ratio of 2.8 was measured in AES. The same structural properties imply a similar stoichiometry of the films while the Auger ratio implies an increased oxygen concentration at the surface. These observations may be explained if Sn that was not incorporated in the oxide film (i.e., was alloyed in the Pt substrate) after the first oxidation cycle is now oxidized allowing more oxygen to be bound to the surface.

Repeated dosing and annealing eventually resulted in a surface structure exhibiting a (5×5) LEED pattern. For such a structure the Sn(430 eV):O(510 eV) ratio was further reduced to a value of 2.3, indicating a more fully oxidized tin–oxide film. STM images show islands arranged on a (5×5) net with respect to the Pt(111) surface and separated by narrow gaps (~0.1–0.2 nm). These islands were uniformly distributed over the whole surface, as is apparent in Fig. 1(c). The islands themselves have an irregular shape and no crystalline island substructure could be imaged with the STM. This, and the lack of any additional LEED spots, apart from the (5×5) spots, implies that the islands are only weakly ordered or in a glassy state. The corrugation of the islands in STM images was 0.1–0.2 nm [Fig. 1(d)], where the lower value is likely to be a tip artifact due to the narrowness of the gap between the islands.

The observed corrugation was independent of the bias voltage applied over the range of 30–800 mV. The observed features in STM are thus attributed to large regions of well-ordered arrays of nanodots, separated by gaps of about the width of one dot. These larger gaps have the same height as the gaps between the dots in the arrays. Such features can easily be explained by regions that expose the substrate and the main features of the image are topographic features. Consequently, we conclude that the dots are topographic features separated by gaps reaching to the substrate. Although electronic effects in STM measurements, in particular on oxide surfaces, can give rise to apparent height differences of 0.1 mm[15,16] and oxide films can even appear ''transparent'' if imaged at bias voltages significantly below the band gap of the oxide film,[17] these effects do not appear to be important for the system studied here. This is not surprising because even bulk SnO_2 is a semiconductor and not an insulator, and more importantly, x-ray photoemission spectroscopy studies of ultrathin SnO_x films on Pt(111) show that Sn exists in a ''quasimetallic'' state and not in a Sn^{2+} or even Sn^{4+} state.[18] Consequently, we expect the SnO_x nanodots to have metallic properties and thus to be less susceptible to electronic effects. Weaker electronic effects may, however, contribute to an underestimation of the corrugation of the dots. This is because the tunneling probability is likely to be higher between the STM tip and a metal (platinum substrate), than between the tip and an oxide (SnO_x islands). The islands arrange perfectly on a (5×5) net, even though there are numerous ''defects'' in this superlattice. Rows of SnO_x islands are sometimes missing, and individual islands are smaller, or missing entirely, but the overall superlattice does not appear to be influenced by these defects. Thus, the island structure displays a ''crystal-like'' two-dimensional superlattice, manifested in the sharp (5×5) LEED pattern.

The intermediate structure that forms following reoxida-

tion and annealing of the (4×4) structure [Fig. 1(b)], has features similar to the (5×5) island structure. Some of the LEED spots are (5×5) spots and the row-like pattern in the STM images have a periodicity five times the Pt surface lattice constant if measured at a 60° angle to the rows, i.e., in the low index direction of the Pt substrate. This indicates that the intermediate structure in Fig. 1(b) is closely related to the (5×5) island structure in Fig. 1(c). Incomplete oxidation of Sn in the intermediate structure may allow the overlayer to partly relax and to ''break up'' in only one dimension to form rows as observed by STM. Three domains have been observed on the surface with the rows rotated by 60°. The brighter ''spots'' in STM images along these rows may indicate the onset of island formation. Their minimum separation along the rows corresponds to five Pt(111) unit cell distances, and neighboring spots on adjacent rows often form a 60° angle to the rows, and thus adopt the hexagonal symmetry of the (5×5) island structure.

The proposed ordering of disordered islands in an ordered superlattice may appear surprising. However, the formation of amorphous oxide layers on metal substrates is commonly observed,[19] and for example was also found for SnO_x on Au(111).[20] The Pt(111) substrate is known to promote SnO_x overlayer decomposition due to strong Sn–Pt interaction.[21,22] We speculate that this strong interaction results in preferred Sn sites on the Pt surface, which in turn may be responsible for the ordering of the SnO_x islands. Even for amorphous materials, a ''local-order condition'' exists that manifests itself in preferential neighbor distances. For amorphous SnO_2 nanoparticles, a Sn–O distance of ~0.21 nm and a Sn–Sn distance of ~0.33 nm was measured.[23] This can be compared to the surface lattice distance for Pt(111) of 0.278 nm. The ordering of the oxygen deficient surface into a (4×4) pattern is consistent with population of preferred sites on the Pt(111) surface by oxidized Sn adatoms. Although further oxidation disrupts this order, one expects that there is still a tendency for Sn to occupy these low energy sites. Competition exists between the interaction of the Sn oxide with the Pt substrate and the interactions within the oxide adlayer and this may result in a considerably strained oxide film. The stress in this film can be (partly) relieved by the formation of small islands. This is similar to the fragmentation of large, uniformly strained, Ag islands on Pt(111) into small islands upon annealing of the sample.[24] Thus, we propose that the formation of the (5×5) superlattice occurs as a result of stress minimization. The observed order is a consequence of the breaking up of a continuous overlayer via the formation of a regular dislocation network. An indication of the formation of such a dislocation network is the intermediate structure shown in Fig. 1(b) that exhibits rows with the same periodicity as the (5×5) island structure in one direction. Fully oxidizing this surface appears to break up these rows into the observed islands. These results demonstrate that oxidation of an adlayer on a metal substrate may result in self-formation of a periodic lateral superlattice on a molecular length scale that is stable up to elevated temperatures.

This work was supported by the National Science Foundation (NSF), Chemistry Division, Surface and Analytical Chemistry Division. One of the authors (M.B.) acknowledges financial support from the Deutsche Forschungsgemeinschaft (DFG).

[1] V. A. Shchukin and D. Bimberg, Rev. Mod. Phys. **71**, 1125 (1999).
[2] H. Brune, H. Röder, C. Boragno, and K. Kern, Phys. Rev. B **49**, 2997 (1994).
[3] L. P. Zhang, J. van Ek, and U. Diebold, Phys. Rev. B **59**, 5837 (1999).
[4] H. Bethge, D. Heuer, Ch. Jensen, K. Reshöft, and U. Köhler, Surf. Sci. **331**, 878 (1995).
[5] H. Brune, M. Giovannini, K. Bromann, and K. Kern, Nature (London) **394**, 451 (1998).
[6] K. Bromann, M. Giovannini, H. Brune, and K. Kern, Eur. Phys. J. D **9**, 25 (1999).
[7] D. D. Chambliss, R. J. Wilson, and S. Chiang, Phys. Rev. Lett. **66**, 1721 (1991).
[8] L. Vitali, M. G. Ramsey, and F. P. Netzer, Phys. Rev. Lett. **83**, 316 (1999).
[9] R. Franchy, Surf. Sci. Rep. **38**, 195 (2000).
[10] S. A. Chambers, Surf. Sci. Rep. **39**, 105 (2000).
[11] H.-J. Freund, H. Kuhlenbeck, and V. Staemmler, Rep. Prog. Phys. **59**, 283 (1996).
[12] F. Mugele, C. Kloos, and P. Leiderer, Rev. Sci. Instrum. **67**, 2557 (1996).
[13] M. T. Paffett and R. G. Windham, Surf. Sci. **208**, 34 (1989).
[14] C. Xu and B. E. Koel, Surf. Sci. **310**, 198 (1994).
[15] G. S. Herman, M. C. Gallagher, S. A. Joyce, and C. H. F. Peden, J. Vac. Sci. Technol. B **14**, 1126 (1996).
[16] U. Diebold, J. Lehman, T. Mahmoud, M. Kuhn, G. Leonardelli, W. Hebenstreit, M. Schmid, and P. Varga, Surf. Sci. **411**, 137 (1998).
[17] T. Bertrams, A. Brodde, and H. Neddermeyer, J. Vac. Sci. Technol. B **12**, 2122 (1994).
[18] M. Batzill, D. E. Beck, D. Jerdev, and B. E. Koel, J. Vac. Sci. Technol. A (in press).
[19] G. H. Vurens, M. Salmeron, and G. A. Somorjai, Prog. Surf. Sci. **32**, 211 (1989).
[20] Y. Zhang and A. J. Slavin, J. Vac. Sci. Technol. A **10**, 2371 (1992).
[21] S. D. Gardener, G. B. Hoflund, M. R. Davidson, and D. R. Schryer, J. Catal. **115**, 2460 (1992).
[22] N. A. Saliba, Y. L. Tsai, and B. E. Koel, J. Phys. Chem. B **103**, 1532 (1999).
[23] V. M. Jimenez, A. Caballero, A. Fernandez, J. P. Espinós, M. Ocaña, and A. R. González-Elipe, Solid State Ionics **116**, 117 (1999).
[24] A. F. Becker, G. Rosenfeld, B. Poelsema, and G. Comsa, Phys. Rev. Lett. **70**, 477 (1993).